Two-photon exchange corrections to $\gamma^* N\Delta$ form factors for $Q^2 \leqslant 4$ (GeV/c)^2

Hai-Qing Zhou[1] and Shin Nan Yang[2]
[1]*Department of Physics, Southeast University, NanJing 211189, China*
[2]*Department of Physics and Center for Theoretical Sciences, National Taiwan University, Taipei 10617, Taiwan*
(Received 15 April 2017; revised manuscript received 6 September 2017; published 28 November 2017)

We evaluate the corrections of the two-photon exchange (TPE) process on the $\gamma^* N\Delta$ transition form factors. The contributions of the TPE process to $eN \to e\Delta(1232) \to eN\pi$ are calculated in a hadronic model with the inclusion of only the elastic nucleon intermediate states, to estimate its effects on the multipoles $M_{1^+}^{(3/2)}$, $E_{1^+}^{(3/2)}$, $S_{1^+}^{(3/2)}$ at the Δ peak. We find that TPE effects on G_M^* are very small. G_E^*, and G_C^* are also little affected at small Q^2. For G_E^*, the TPE effects reach about 3–8% near $Q^2 \sim 4$ GeV^2, depending on the model, MAID or SAID, used to emulate the data. For G_C^*, the TPE effects decrease rapidly with increasing ϵ while growing with increasing Q^2 to reach $\sim$ 6–15% with $Q^2 \sim 4$ GeV^2 at $\epsilon = 0.2$. Sizeable TPE corrections to G_E^* and G_C^* found here point to the need to include TPE effects in the multipole analysis in the region of high Q^2 and small ϵ. The TPE corrections to R_{EM} and R_{SM} obtained in our hadronic calculation are compared with those obtained in a partonic calculation for moderate momentum transfer of $2 < Q^2 < 4$ GeV^2.

DOI: 10.1103/PhysRevC.96.055210

I. INTRODUCTION

The Jones-Scadron form factors—magnetic dipole G_M^*, electric quardrupole G_E^*, and Coulomb quardrupole G_C^*—which describe the electromagnetic transition between the first two lowest baryon states, the nucleon and the $\Delta(1232)$ resonances, are of fundamental interest. They are proportional to the three multipoles $M_{1^+}^{(3/2)}$, $E_{1^+}^{(3/2)}$, $S_{1^+}^{(3/2)}$ at the resonance peak [1], which are all purely imaginary. Namely, on the resonance peak $W = M_\Delta$, one has

$$\begin{aligned} G_M^* &= N \,\mathrm{Im}\, M_{1^+}^{(3/2)}(Q^2, W = M_\Delta), \\ G_E^* &= -N \,\mathrm{Im}\, E_{1^+}^{(3/2)}(Q^2, W = M_\Delta), \\ G_C^* &= -\left(\frac{2M_\Delta}{q_\Delta}\right) N \,\mathrm{Im}\, S_{1^+}^{(3/2)}(Q^2, W = M_\Delta), \end{aligned} \tag{1}$$

where $N = \frac{8}{e}\left(\frac{\pi k_\Delta M_\Delta \Gamma_\Delta}{3 q_\Delta}\frac{Q_+}{Q_-}\right)^{1/2}\left(\frac{M_N}{M_N + M_\Delta}\right)$, with $e^2/4\pi \simeq 1/137$, $Q_\pm \equiv [(M_\Delta \pm M_N)^2 + Q^2]^{1/2}$, Γ_Δ is the Δ width, and M_N and M_Δ are the nucleon and Δ masses, respectively. q_Δ and k_Δ denote the magnitudes of the virtual photon and pion three-momenta in the Δ rest frame at the resonance position, respectively.

At sufficiently large four-momentum transfer squared, Q^2, perturbative QCD (pQCD) predicts that only helicity-conserving amplitudes contribute [2], leading to G_M^*, G_E^*, and G_C^* scaling as Q^{-4}, Q^{-4}, and Q^{-6}, respectively. It follows that

$$\begin{aligned} R_{EM} &\equiv \left(E_{1^+}^{(3/2)}/M_{1^+}^{(3/2)}\right)\Big|_{W=M_\Delta} = -G_E^*/G_M^* \to 1, \\ R_{SM} &\equiv \left(S_{1^+}^{(3/2)}/M_{1^+}^{(3/2)}\right)\Big|_{W=M_\Delta} \\ &= -(Q_+ Q_-/4M_\Delta^2)(G_C^*/G_M^*) \to \text{const.} \end{aligned} \tag{2}$$

In the nonpertubative regime with low Q^2, a symmetric SU(6) quark model would allow the electromagnetic excitation of the Δ to proceed only via $M1$ transition. However, the tensor component of the one-gluon exchange interaction between quarks would induce a D state in the Δ, which leads to a deformed Δ, and the photon can excite a nucleon through electric $E2$ and Coulomb $C2$ quardrupole transitions, resulting in nonvanishing $E_{1^+}^{(3/2)}$ and $S_{1^+}^{(3/2)}$ multipoles. Experiments give, near $Q^2 = 0$, $R_{EM} = -(2.5 \pm 0.5)\%$ [3], a clear indication of Δ deformation. Below $Q^2 \leqslant 6$ Gev^2, R_{EM} remains small and negative, while R_{SM} continues to become more negative with increasing Q^2, indicating that the pQCD limit is nowhere in sight. The intriguing difference in the behaviors of the R_{EM} in the perturbative and nonperturbative domains remains to be understood.

The multipoles are extracted from pion electroproduction experiments based on the one-photon exchange (OPE) approximation. The OPE approximation has been widely used to analyze most of the electromagnetic nuclear reactions. The validity of the OPE approximation has recently been under heavy scrutiny [4–6]. It was prompted by the substantial difference in the ratio of proton electric and magnetic form factors extracted from ep elastic scattering via the Rosenbluth technique [7,8] and polarization transfer measurements [9–11], for $Q^2 < 6$ GeV^2. The two-photon exchange (TPE) corrections as estimated by hadronic and partonic calculations show that TPE effects can account for more than half of that discrepancy.

It is hence important to determine how much TPE effects would affect the extraction of multipoles from pion electroproduction. Specifically we will be concerned with only the multipoles related to the $N\Delta$ transition in this study; namely, how the extraction of $M_{1^+}^{(3/2)}$, $E_{1^+}^{(3/2)}$, and $S_{1^+}^{(3/2)}$, or equivalently the transition form factors, would be affected in the presence of TPE. This question was addressed in [12], where a partonic approach, with the use of $N\Delta$ generalized parton distributions, was employed to estimate the TPE effects. For $2 < Q^2 < 4$ GeV^2 at $\epsilon = 0.2$, they found that the TPE corrections on R_{EM} and R_{SM} are small, lying in the range $-(0.2$–$0.6)\%$. However, it is known that the partonic approach is applicable only for Q^2 large comparable to a typical hadronic scale and becomes questionable for Q^2, which in the current case is less than $\sim$ 2–3 GeV^2. In this lower Q^2 region, the

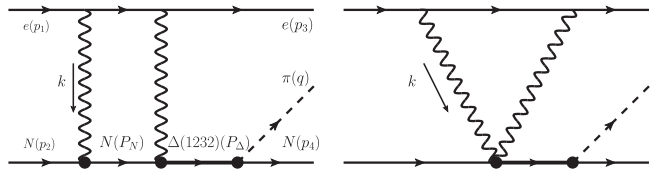

FIG. 1. TPE box (a) and contact (b) diagrams for $eN \to e\Delta \to eN\pi$. The cross-box diagram is not shown.

hadronic approach as developed in [13] would be more reliable, which motivates this investigation.

II. TWO-PHOTON EXCHANGE CORRECTIONS TO THE CROSS SECTION

In this work, we present results of a hadronic calculation of the TPE corrections, as depicted in Fig. 1, where only the elastic N intermediate states are considered, to the process $eN \to eN\pi$ on the Δ peak. The intermediate nucleons are assumed to be on-mass-shell, which is justified in the study of TPE effects in ep elastic scatterings within hadronic approach in [13].

As in [14–16], we choose the Feynman gauge and neglect electron mass m_e in the numerators to obtain the amplitude of the box diagram in Fig. 1(a) as

$$\mathcal{M}^{2\gamma,a} = -i\int \frac{d^4k}{(2\pi)^4}\bar{u}(p_3)\Gamma^{\gamma ee}_{\mu}S^{(e)}(p_1-k)\Gamma^{\gamma ee}_{\nu}u(p_1) \times\frac{-i}{k^2+i\varepsilon}\frac{-i}{(P_\Delta-P_N)^2+i\varepsilon}\bar{u}(p_4)\Gamma^{\pi N\Delta,\alpha}(q)S^{(\Delta)}_{\alpha\beta}(P_\Delta) \times\Gamma^{\mu\beta}_{\gamma N\to\Delta}(P_\Delta,P_\Delta-P_N)S^{(N)}(P_N)\Gamma^{\gamma NN,\nu}(k)u(p_2), \tag{3}$$

where $\Gamma^{\gamma ee}_{\mu} = -ie\gamma_\mu$, and $\Gamma^{\gamma NN}_{\mu} = ie\langle P(p')|J^{em}_{\mu}|P(p)\rangle$ is the proton electromagnetic current matrix element. $\Gamma^{\pi N\Delta,\alpha}(q) = (f_{\pi N\Delta}/m_\pi)q^\alpha T^\dagger$ denotes the $\pi N\Delta$ transition vertex function with $f^2_{\pi N\Delta}/4\pi = 0.36$ and $T^\dagger$ the isospin $1/2 \to 3/2$ transition operator. $S^{(e,N,\Delta)}$ denote the propagators of electron, proton, and Δ, respectively, as specified by the superscript. The forms of the $S^{(\Delta)}$ and the $\gamma N \to \Delta$ transition vertex function $\Gamma^{\mu\beta}_{\gamma N\to\Delta}$ can be found in [16]. The realistic form factors are used for $\Gamma^{\gamma NN}_{\mu}$ and $\Gamma^{\mu\beta}_{\gamma N\to\Delta}$ as in [15,16]. Amplitude for the cross-box diagram can be written down similarly. A contact term $M^{2\gamma,ct}$, as depicted in Fig. 1(b), is needed because of the requirement of current conservation. Following the prescription suggested in [17], we obtain

$$\mathcal{M}^{2\gamma,ct} = -i\int \frac{d^4k}{(2\pi)^4}\bar{u}(p_3)\Gamma^{\gamma ee}_{\mu}S^{(e)}(p_1-k)\Gamma^{\gamma ee}_{\nu}u(p_1) \times\frac{-i}{k^2+i\varepsilon}\frac{-i}{(P_\Delta-P_N)^2+i\varepsilon}\bar{u}(p_4)\Gamma^{\pi N\Delta,\alpha}(q)S^{(\Delta)}_{\alpha\beta}(P_\Delta) \times\Gamma^{\mu\nu\beta}_{\gamma\gamma N\Delta}(P_\Delta,p_2,k,p_4-p_2-k)u(p_2), \tag{4}$$

with

$$\Gamma^{\mu\nu\beta}_{\gamma\gamma N\Delta}(P_\Delta,p_2,k,\bar{k}) = e\left\{(2p_2+k)^\nu\frac{F_1(k)}{(p_2+k)^2-M_N^2}\Gamma^{\mu\beta}_{\gamma N\to\Delta}(P_\Delta,\bar{k}) +(2p_2+\bar{k})^\mu\frac{F_1(\bar{k})}{(p_\Delta-k)^2-M_N^2}\Gamma^{\nu\beta}_{\gamma N\to\Delta}(P_\Delta,k)\right\}, \tag{5}$$

where $\bar{k} = p_4 - p_2 - k$, and F_1 is the Dirac form factor of the nucleon. The inclusion of the contact term of Eq. (4) makes the full amplitude gauge invariant as discussed in [17]. We have also checked numerically that the full amplitude does not dependent on the gauge parameter. It is also essential to ensure the sum to be free of IR divergence. The packages FEYNCALC [18] and LOOPTOOLS [19] are used to carry out the analytical and numerical calculations, respectively.

Within the OPE approximation, the fivefold $eN \to eN\pi$ differential cross section, with both unpolarized initial and final states, can be expressed as $d^5\sigma^{1\gamma}/d\Omega_f dE_f d\Omega_\pi \equiv \Gamma d\sigma^{1\gamma}/d\Omega_\pi$, with Γ the virtual photon flux factor and

$$\frac{d\sigma^{1\gamma}}{d\Omega_\pi} = \left\{\sigma_0^{1\gamma} + \sqrt{2\epsilon(1+\epsilon)}\sigma_{LT}^{1\gamma}\cos\phi + \epsilon\sigma_{TT}^{1\gamma}\cos 2\phi\right\}, \tag{6}$$

where $\sigma_0^{1\gamma} = \sigma_T^{1\gamma} + \epsilon\sigma_L^{1\gamma}$ and ϵ is the transverse polarization of the virtual photon. The superscript 1γ is used to emphasize that the quantities are defined within the OPE approximation scheme, a convention to be followed hereafter. E_f, Ω_f denote the energy and solid-angle of the scattered electron in the laboratory frame, respectively, and ϕ is the tilt angle between the electron scattering plane and the reaction plane, $d\Omega_\pi$ is the pion solid-angle differential measured in the center-of-mass (c.m.) frame of the final pion and nucleon.

The OPE differential cross sections $\sigma^{1\gamma}_{T,L,LT,TT}$ are all functions of multipoles, which depend on W, Q^2, and pion polar angle θ_π in the πN c.m. frame, but are ϵ independent. The multipoles are determined in multipole analysis, e.g., MAID [20] or SAID [21], by fitting the experimental data as

$$\frac{d\sigma^{ex}}{d\Omega_\pi} \simeq \frac{d\sigma^{1\gamma}}{d\Omega_\pi} = C\left|\mathcal{M}^{1\gamma}\left(X^{1\gamma}_{1^+}, Z^{1\gamma}_{l^\pm}\right)\right|^2, \tag{7}$$

where $d\sigma^{ex}/d\Omega_\pi$ is measured experimentally. Here $X^{1\gamma}_{1^+} = (M^{(3/2),1\gamma}_{1^+}, E^{(3/2),1\gamma}_{1^+}, S^{(3/2),1\gamma}_{1^+})$ denote the multipoles pertaining to the Δ excitation channel of $(3/2, 3/2)$, $Z^{1\gamma}_{l^\pm}$ represents all other multipoles, and C is a kinematical factor.

With the TPE effects included, the analysis of the experimental data should be performed by using

$$\frac{d\sigma^{ex}}{d\Omega_\pi} \simeq \frac{d\sigma^{1\gamma+2\gamma}}{d\Omega_\pi} = C\left\{\left|\mathcal{M}^{1\gamma}\left(X^{1\gamma+2\gamma}_{1^+}, Z^{1\gamma+2\gamma}_{l^\pm}\right)\right|^2 +2\,\mathrm{Re}\left[\mathcal{M}^{1\gamma *}\left(X^{1\gamma+2\gamma}_{1^+}, Z^{1\gamma+2\gamma}_{l^\pm}\right)\mathcal{M}^{2\gamma}\right]\right\}, \tag{8}$$

where the term $|\mathcal{M}^{2\gamma}|^2$ has been neglected. $(X^{1\gamma+2\gamma}_{1^+}, Z^{1\gamma+2\gamma}_{l^\pm})$ are the multipoles determined from the OPE plus TPE approximation of Eq. (8), as referred to by the superscript

$1\gamma + 2\gamma$, a notation to be followed hereafter. Obviously, they must deviate from ($X_{1^+}^{1\gamma}$, $Z_{l^\pm}^{1\gamma}$) of Eq. (7) based on the OPE. Equation (6) still holds for $d\sigma^{1\gamma+2\gamma}/d\Omega_\pi$ but the cross sections $\sigma_{T,L,LT,TT}^{1\gamma+2\gamma}$ would become ϵ dependent [1,12].

III. TWO-PHOTON EXCHANGE CORRECTIONS TO THE MULTIPOLES

In principle, one should try to determine the multipoles $X_{1^+}^{1\gamma+2\gamma}$ and $Z_{l^\pm}^{1\gamma+2\gamma}$ in the presence of TPE by fitting the data with Eq. (8). The obtained values of the multipoles would represent the genuine multipoles as would be defined within the OPE approximation scheme, with TPE effects removed, from the data.

Extraction of $X_{1^+}^{1\gamma+2\gamma}$'s and $Z_{l^\pm}^{1\gamma+2\gamma}$'s from data via Eq. (8) is beyond the scope of the present study. To proceed, two approximations will be made. First, we assume that only the multipoles $X_{1^+}^{1\gamma+2\gamma}$ will be much affected in the presence of the TPE depicted in Fig. 1. This can be justified because the final πN pair there arose only from the decay of Δ and would be in the state with ($J = 3/2$, $I = 3/2$) only. The multipoles $Z_{l^\pm}^{1\gamma+2\gamma}$ will then be taken to be unchanged and fixed, i.e., $Z_{l^\pm}^{1\gamma+2\gamma} = Z_{l^\pm}^{1\gamma}$, and Eq. (8) is reduced to depend only on the three multipoles $X_{1^+}^{1\gamma+2\gamma}$. The Fermi-Watson theorem requires that these three multipoles should all have the phase given by the πN P_{33} phase shift, which is $\pi/2$ on the Δ peak. So the three multipoles $X_{1^+}^{1\gamma+2\gamma}$ will all become purely imaginary in Eq. (8). Hereafter, X_{1^+} will be taken to denote the imaginary part of $X_{1^+}^{1\gamma+2\gamma}$ for brevity.

Eq. (8) is then simplified to

$$\frac{d\bar{\sigma}^{ex}}{d\Omega_\pi} \equiv \frac{d\sigma^{ex}}{d\Omega_\pi} - 2C\,\mathrm{Re}[\mathcal{M}^{1\gamma *}(X_{1^+})\mathcal{M}^{2\gamma}] = C|\mathcal{M}^{1\gamma}(X_{1^+})|^2, \tag{9}$$

where a TPE-corrected cross section $d\bar{\sigma}^{ex}/d\Omega_\pi$ is introduced. Dependence on $Z_{l^\pm}$'s in $\mathcal{M}^{1\gamma}$ in Eq. (9) is not shown for simplicity since they remain fixed. We like to emphasize here that the $\sigma_{T,L,LT,TT}^{ex}$'s are in principle ϵ dependent. Only precisely determined $d\sigma^{ex}/d\Omega_\pi$'s and a complete theory for $\mathcal{M}^{2\gamma}$ would lead to ϵ-independent $\bar{\sigma}_{T,L,LT,TT}^{ex}$'s. $d\bar{\sigma}^{ex}/d\Omega_\pi$ is only then expressible in the form of $|\mathcal{M}^{1\gamma}|^2$.

To proceed, we approximate the data $d\sigma^{ex}/d\Omega_\pi$ with the use of one of the existing $eN \to eN\pi$ models, MAID [20] or SAID [21], to be denoted as $\sigma_{T,L,LT,TT}^{MAID/SAID}$. There is a caveat here with such an approximation. All existing models, like MAID and SAID, are based on the OPE approximation, and the resulting cross sections $\sigma_{T,L,LT,TT}^{1\gamma}$ and multipoles would hence be ϵ independent. Approximating ϵ-dependent $\sigma_{T,L,LT,TT}^{ex}$'s by ϵ-independent $\sigma_{T,L,LT,TT}^{MAID/SAID}$'s would give rise to X_{1^+}'s determined from Eq. (9) to be ϵ dependent.

Once $d\sigma^{ex}/d\Omega_\pi$ is given, Eq. (9) then can be solved for $X_{1^+}^{1\gamma}$'s by iteration via

$$\frac{d\bar{\sigma}^{ex,i+1}}{d\Omega_\pi} \equiv \frac{d\sigma^{ex}}{d\Omega_\pi} - 2C\,\mathrm{Re}\left[\mathcal{M}^{1\gamma *}\left(X_{1^+}^{i}\right)\mathcal{M}^{2\gamma}\right] = C\left|\mathcal{M}^{1\gamma}\left(X_{1^+}^{i+1}\right)\right|^2. \tag{10}$$

We start with values of multipoles given by MAID or SAID, i.e., $X_{1^+}^{0} = X_{1^+}$(MAID/SAID) in the first iteration $i = 0$, depending on which model is employed to approximate $d\sigma^{ex}/d\Omega_\pi$ in Eq. (9). It should be noted that both the left- and right-hand sides depend on θ_π and ϕ.

Next, we have to determine the three multipoles $X_{1^+}^{i+1}$'s from Eq. (10) for fixed Q^2 and ϵ at the i-th iteration. Upon first glance, one could in principle write down three equations for each of the $\sigma_{0,LT,TT}$'s and solve for the three variables X_{1^+}'s. These three equations are all quadratic equations in X_{1^+}'s. It turns out that there are a few angles where no real solutions exist for this coupled algebraic equations. The solutions show rapid variations *w.r.t.* θ_π in the neighbourhood of these angles. The reason can be traced to the approximation we make to replace $d\sigma^{ex}/d\Omega_\pi$ by $(d\sigma^{ex}/d\Omega_\pi)$(MAID/SAID) in (10).

We hence turn to least-square method. As reported in [22], results obtained with such minimization procedure show strong sensitivity to the angle-independent weights attached to each of the three cross sections $\sigma_{0,LT,TT}$'s. We now understand that this sensitivity arises from the problem described in the last paragraph. Accordingly, we decide to follow the fitting method adapted in MAID [20]. At the i-th iteraction, we minimize $\chi^2(Q^2,\epsilon)$ defined as

$$\chi_i^2(Q^2,\epsilon) \equiv \sum_{\theta_\pi,\phi}\left(\frac{\mathcal{N}_{i+1}}{\delta d\sigma^{ex}(\theta_\pi,\phi)}\right)^2, \tag{11}$$

with

$$\mathcal{N}_{i+1} = \left[d\bar{\sigma}^{ex,i+1}(\theta_\pi,\phi) = C\left|\mathcal{M}^{1\gamma}\left(X_{1^+}^{i+1}\right)\right|^2\right] - \left[\frac{d\sigma^{ex}}{d\Omega_\pi} - 2C\,\mathrm{Re}\left[\mathcal{M}^{1\gamma *}\left(X_{1^+}^{i}\right)\mathcal{M}^{2\gamma}\right]\right], \tag{12}$$

where $d\sigma^{ex}/d\Omega_\pi = (d\sigma^{ex}/d\Omega_\pi)$(MAID/SAID). $X_{1^+}^{i}$'s are kept fixed while $X_{1^+}^{i+1}$'s are varied in the minimization of χ_i^2. In Eq. (12) $\delta d\sigma^{ex}(\theta_\pi,\phi)$ is the total error of $d\sigma^{ex}(\theta_\pi,\phi)$, which also depends on Q^2 and ϵ. In our analysis, the experimental errors at $Q^2 = 2.8\,\mathrm{GeV}^2, \epsilon = 0.56$ and $Q^2 = 4\,\mathrm{GeV}^2, \epsilon = 0.5$ provided in [23] are used. Either set of errors gives rise to nearly identical results. We choose to use the ones at $Q^2 = 2.8$ GeV^2, $\epsilon = 0.56$ for all other values of Q^2 and ϵ considered.

IV. RESULTS AND DISCUSSIONS

We will show only the ratios $X_{1^+}^{1\gamma+2\gamma}/X_{1^+}^{1\gamma} \equiv G^{*,1\gamma+2\gamma}/G^{*,1\gamma}$ between the TPE-corrected or the genuine OPE values $X_{1^+}^{1\gamma+2\gamma}$ ($\propto G^{*,1\gamma+2\gamma}$) obtained here, and the input OPE values $X_{1^+}^{1\gamma}$ ($\propto G^{*,1\gamma}$) given by the models (MAID, SAID) used to emulate the experimental data. They will be labeled as MAID and SAID, respectively. Results for $M_{1^+}^{3/2}$ will not be shown as the TPE effects on it are found to be very small with both models. We do not show results above $Q^2 > 4$ GeV^2 as the validity of hadronic approach adopted here might be questionable in the high-Q^2 region. The results obtained with MAID and SAID are presented for $0 < \epsilon < 0.9$ at $Q^2 = 0.127$ and 2.8 GeV^2 in Fig. 2 and for $0 < Q^2 < 4$ GeV^2 with $\epsilon = 0.2$ and 0.5 in Fig. 3. The results with MAID are denoted by the solid and dotted (red) curves,

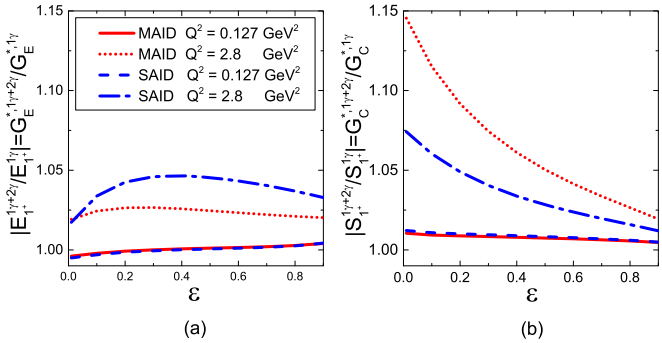

FIG. 2. The TPE corrections to $E_{1^+}^{(3/2)}$ and $S_{1^+}^{(3/2)}$ vs ϵ at fixed Q^2. The labels MAID and SAID are used to indicate that the results are obtained with using either MAID or SAID to emulate the experimental cross sections, respectively, as explained in the text. The solid and dotted curves (red) refer to the results with MAID, and the dashed and dashed-dotted curves (blue) denote the results with SAID.

while the results with SAID are denoted by the dashed and dashed-dotted (blue) curves, respectively.

In Fig. 2, one sees that at small $Q^2 = 0.127$ GeV^2 the TPE corrections to both $E_{1^+}^{3/2}(G_E^*)$ and $S_{1^+}^{3/2}(G_C^*)$ are less than 1% and stay flat for all values of ϵ, irrespective of the model used. As Q^2 grows, TPE effects begin to increase and dependence on the model used develops. For $E_{1^+}^{3/2}(G_E^*)$, the TPE corrections eventually reach about 3% and 8% at 4 GeV^2 in the case of MAID and SAID, respectively, as seen in Fig. 3(a), with mild sensitivity with respect to ϵ. The TPE corrections to $S_{1^+}^{3/2}(G_C^*)$ at $Q^2 = 2.8$ GeV^2, as depicted in Fig. 2(b), show considerable sensitivity not only to model but also ϵ, decreasing from around 7.5% and 15% near $\epsilon = 0$, for SAID and MAID, respectively, to only 2% as ϵ approaches 0.9. Figure 3(b) shows how TPE corrections for $S_{1^+}^{3/2}(G_C^*)$ grow with increasing Q^2 to reach about 15% and 6%, respectively, at $\epsilon = 0.2$ and $Q^2 = 4$ GeV^2, for MAID and SAID. Sizeable TPE corrections to $E_{1^+}^{3/2}(G_E^*)$ and $S_{1^+}^{3/2}(G_C^*)$ found here point to the need to include TPE effects in the multipole analysis of data in the region of high Q^2 and small ϵ.

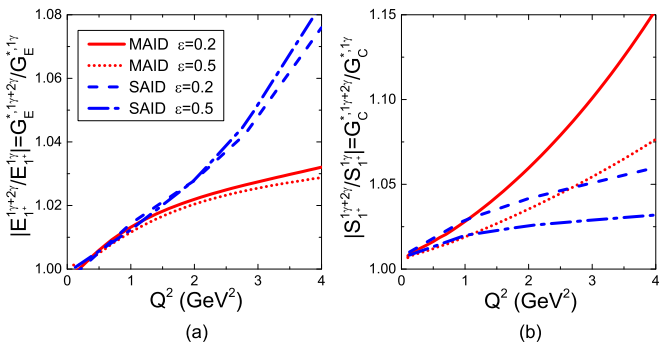

FIG. 3. The TPE corrections to $E_{1^+}^{(3/2)}$ and $S_{1^+}^{(3/2)}$ vs Q^2 at fixed ϵ. The notation is the same as in Fig. 2.

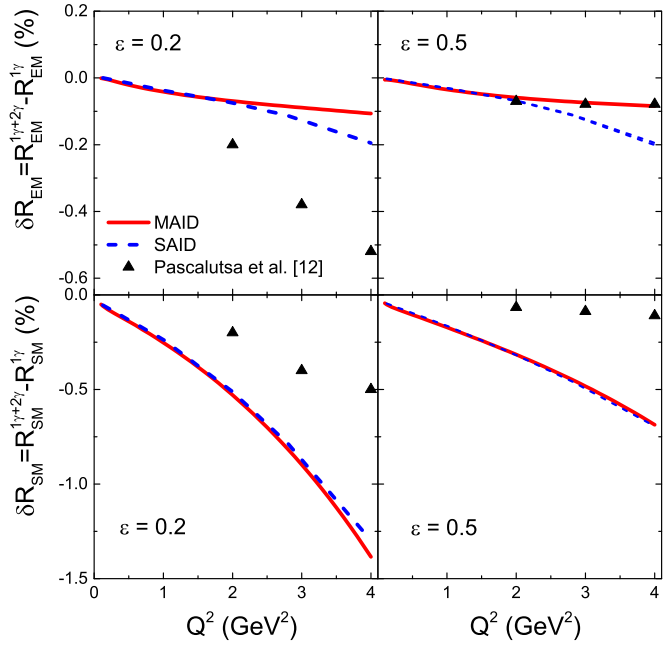

FIG. 4. The TPE corrections to the extracted R_{EM} and R_{SM} vs Q^2 at fixed ϵ. The notation for curves is the same as in Fig. 2. The black triangles denote the results of the partonic calculation of [12].

It is straightforward to obtain the values for the TPE-corrected ratios $R_{EM,SM}^{1\gamma+2\gamma}$ from the results presented in Fig. 3. The differences $\delta R_{EM,SM}$ between $R_{EM,SM}^{1\gamma+2\gamma}$ and the model ratios $R_{EM,SM}^{1\gamma}$, i.e., $\delta R_{EM} \equiv R_{EM}^{1\gamma+2\gamma} - R_{EM}^{1\gamma}$ and $\delta R_{SM} = R_{SM}^{1\gamma+2\gamma} - R_{SM}^{1\gamma}$, for $0 < Q^2 < 4$ GeV^2 are shown in Fig. 4, where the solid (red) and dashed (blue) curves refer to the results obtained with MAID and SAID, respectively. We first note that the TPE corrections $\delta R_{EM,SM}$ are almost equal with the two models except for δR_{EM} when $Q^2 > 2$ GeV^2. This is in contrast to Figs. 2 and 3 where model dependence grows rapidly with increasing Q^2 after $Q^2 \sim 1$ GeV^2. For both $\epsilon = 0.2$ and 0.5, δR_{EM} is negligible for small Q^2 and becomes more negative toward -0.1% and -0.2% when Q^2 approaches $Q^2 = 4$ GeV^2, in the cases of MAID and SAID, respectively. The TPE effect for δR_{SM} is considerably larger than for δR_{EM}. It also starts near zero for $Q^2 \sim 0$ but decreases rapidly to reach $\sim -1.4\%$ and $\sim -0.7\%$, for $\epsilon = 0.2$ and 0.5, respectively. Magnitude-wise, they are comparable to the current experimental errors [24].

The results of the partonic calculation of [12] for $\delta R_{EM/SM}$'s, denoted by black triangles, are included in Fig. 4 for comparison. The regions of validity of the hadronic and partonic approaches are known to be different except for possible overlap in the range $2 < Q^2 < 4$ GeV^2. It is easily seen that, in this region, our results for δR_{EM} at $\epsilon = 0.2$ obtained with both models are considerably smaller. However, for $\epsilon = 0.5$, our results obtained with MAID almost coincide with those of [12], while results obtained with SAID are distinctly smaller than partonic results. In the case of δR_{SM}, our values are substantially more negative than the partonic results, for both $\epsilon = 0.2$ and 0.5.

The differences between our results and those of [12] for the $R_{EM,SM}$'s as shown in Fig. 4, can be dissected as follows. We first point out that there are two more differences between the two calculations besides the partonic vs hadronic approach. First, only the Δ pole diagram is considered for $\mathcal{M}^{1\gamma}$ in [12], to evaluate the interference effects between OPE and TPE. In other words, the background contribution to $\mathcal{M}^{1\gamma}$, which consists of Born terms and t-channel (ρ, ω) vector-meson exchanges [25], are not included in the evaluation of $\mathrm{Re}[\mathcal{M}^{1\gamma *}\mathcal{M}^{2\gamma}]$ in Eq. (9). In fact, it was found in [26] that both the background terms and the pion cloud effects contribute significantly to $M_{1^+}^{(3/2)}$ and $E_{1^+}^{(3/2)}$ at $Q^2 = 0$. In addition, the truncated multipole expansion (TME) is employed in [12] to estimate the values of $R_{EM,SM}^{1\gamma+2\gamma}$. It is known that the use of the TME and the model fitting used here give rise to a considerable difference in the extraction of $R_{EM,SM}^{1\gamma}$, a feature seen in [27,28].

V. SUMMARY

To summarize, we investigate the effects of two-photon exchange processes in $eN \to e\Delta(1232) \to eN\pi$ in the low Q^2 region, in a hadronic approach. Only the elastic nucleon intermediate states are included in the present study. We focus on the Δ peak to estimate their effects on the $\gamma^* N\Delta$ transition form factors. We emulate the experimental pion electroproduction data with two existing phenomenological models, MAID and SAID. After subtracting out the interference of one-photon and two-photon exchanges from the data, the reminder is used to extract the "genuine" one-photon exchange multipoles $M_{1^+}^{(3/2)}$, $E_{1^+}^{(3/2)}$, $S_{1^+}^{(3/2)}$ at $W = M_\Delta$. This gives us the three $\gamma^* N\Delta$ form factors, G_M^*, G_E^*, and G_C^*, for $0 < Q^2 < 4\ \mathrm{GeV}^2$.

We find that TPE effects on G_M^* are very small. Both G_E^* and G_C^* are also little affected at small $Q^2 < 0.5\ \mathrm{GeV}^2$. However, the TPE effects on G_E^* and G_C^* grow with Q^2, and sensitivity appears with respect to ϵ and the data model used. For G_E^*, the TPE effects reach about 3% and 8% at $Q^2 \sim 4\ \mathrm{GeV}^2$, depending on whether MAID and SAID is used to emulate the data, respectively, with mild dependence on ϵ. For G_C^*, the TPE effects obtained with both MAID and SAID decrease rapidly with increasing ϵ while grow with increasing Q^2, and reach $\sim 15\%$ and $\sim 6\%$ as $Q^2 \to 4\ \mathrm{GeV}^2$ at $\epsilon = 0.2$, respectively, for MAID and SAID. Sizeable TPE corrections to G_E^* and G_C^* found here point to the need to include TPE effects in the multipole analysis of data in the region of high Q^2 and small ϵ.

Our extracted TPE corrections for $\delta R_{EM} \equiv R_{EM}^{1\gamma+2\gamma} - R_{EM}^{1\gamma}$ are very small at $\epsilon = 0.2$ and 0.5, for both MAID and SAID models, up to $Q^2 \leqslant 4.0\ \mathrm{GeV}^2$. This feature is similar to results of the partonic calculation of [12], except our results are only about one third of the magnitude given in [12] for $\epsilon = 0.2$. However, our TPE corrections for R_{SM}, independently of the models used, are considerably larger in magnitude than the results of [12], reaching $\sim -1.4\%$ and $\sim -0.7\%$ for $\epsilon = 0.2$ and 0.5, respectively.

Besides the hadronic vs partonic approach, the differences between our results and those of [12] for $\delta R_{EM/SM}$'s could be attributed to two other simplifications used in [12]. First, in [12] only the Δ pole contribution is included in the OPE amplitude in the evaluation of the interference between OPE and TPE amplitudes. In addition, TME is invoked in the extraction of the ratios $R_{EM/SM}$.

As the TPE effects on G_E^* ($\sim E_{1^+}^{(3/2)}$) and G_C^* ($\sim S_{1^+}^{(3/2)}$) found in this study are not small, more precise measurements on $ep \to e\Delta(1232) \to ep\pi^0$ in the region $2 < Q^2 < 4\ \mathrm{GeV}^2$ will be very desirable. It is important to have data taken for the same Q^2 but at different values of ϵ. The ϵ dependence in the resulting multipoles will be a clear signature of the TPE effects.

We have considered only the elastic nucleon intermediate states in the present study. Similar TPE effects arising from the inclusion of higher resonances like Δ in the intermediate states should be further pursued. TPE effects on the transition form factors of other higher resonances will also be an interesting question to explore.

ACKNOWLEDGMENTS

We thank Dr. Lothar Tiator for helpful communications regarding MAID. We also thank Dr. T.-S.H. Lee for careful reading of the manuscript and suggestions. This work is supported in part by the National Natural Science Foundation of China under Grant No. 11375044, the Fundamental Research Fund for the Central Universities under Grant No. 2242014R30012 for H.Q.Z., and the National Science Council of the Republic of China (Taiwan) for S.N.Y. under Grant No. NSC101-2112-M002-025. H.Q.Z. would like to gratefully acknowledge the support of the National Center for Theoretical Science of the National Science Council of the Republic of China (Taiwan) for his visits in January 2016 and February 2017. He also greatly appreciates the warm hospitality extended to him by the Physics Department of the National Taiwan University during the visits.

[1] V. Pascalutsa, M. Vanderhaeghen, and S. N. Yang, Phys. Rep. **437**, 125 (2007).
[2] S. J. Brodsky, G. P. Lepage, and S. A. A. Zaidi, Phys. Rev. D **23**, 1152 (1981); C. E. Carlson and J. L. Poor, *ibid.* **38**, 2758 (1988).
[3] R. Beck *et al.*, Phys. Rev. Lett. **78**, 606 (1997); G. Blanpied *et al.*, *ibid.* **79**, 4337 (1997).
[4] C. E. Carlson and M. Vanderhaeghen, Annu. Rev. Nucl. Part. Sci. **57**, 171 (2007).
[5] J. Arrington, P. G. Blunden, and W. Melnitchouk, Prog. Nucl. Part. Phys. **66**, 782 (2011).
[6] S. N. Yang, Few-Body Syst. **54**, 45 (2013).
[7] J. Arrington, Phys. Rev. C **68**, 034325 (2003).
[8] I. A. Qattan *et al.*, Phys. Rev. Lett. **94**, 142301 (2005).
[9] M. K. Jones *et al.* (JLab Hall A Collaboration), Phys. Rev. Lett. **84**, 1398 (2000); O. Gayou *et al.* (JLab Hall A Collaboration), *ibid.* **88**, 092301 (2002).
[10] A. J. R. Puckett *et al.*, Phys. Rev. Lett. **104**, 242301 (2010).

[11] X. Zhan *et al.*, Phys. Lett. B **705**, 59 (2011); G. Ron *et al.*, Phys. Rev. C **84**, 055204 (2011).
[12] V. Pascalutsa, C. E. Carlson, and M. Vanderhaeghen, Phys. Rev. Lett. **96**, 012301 (2006).
[13] P. G. Blunden, W. Melnitchouk, and J. A. Tjon, Phys. Rev. Lett. **91**, 142304 (2003); Phys. Rev. C **72**, 034612 (2005); S. Kondratyuk, P. G. Blunden, W. Melnitchouk, and J. A. Tjon, Phys. Rev. Lett. **95**, 172503 (2005).
[14] H. Q. Zhou, C. W. Kao, and S. N. Yang, Phys. Rev. Lett. **99**, 262001 (2007).
[15] H. Q. Zhou, C. W. Kao, S. N. Yang, and K. Nagata, Phys. Rev. C **81**, 035208 (2010).
[16] H. Q. Zhou and S. N. Yang, Eur. Phys. J. A **51**, 105 (2015).
[17] S. Kondratyuk and P. G. Blunden, Nucl. Phys. A **778**, 44 (2006).
[18] R. Mertig, M. Bohm, and A. Denner, Comput. Phys. Commun. **64**, 345 (1991).
[19] T. Hahn and M. Perez-Victoria, Comput. Phys. Commun. **118**, 153 (1999).
[20] D. Drechsel, S. S. Kamalov, and L. Tiator, Euro. Phys. J. A **34**, 69 (2007); http://portal.kph.uni-mainz.de/MAID/maid2007/maid2007.html.
[21] http://gwdac.phys.gwu.edu; L. Tiator, M. Doring, R. L. Workman, M. Hadzimehmedovic, H. Osmanovic, R. Omerovic, J. Stahov, and A. Svarc, Phys. Rev. C **94**, 065204 (2016).
[22] H. Q. Zhou and S. N. Yang, JPS Conf. Proc. **13**, 020040 (2017).
[23] V. V. Frolov *et al.*, Phys. Rev. Lett. **82**, 45 (1999).
[24] M. Ungaro *et al.* (CLAS Collaboration), Phys. Rev. Lett. **97**, 112003 (2006).
[25] S. N. Yang, J. Phys. G **11**, L205 (1985).
[26] S. S. Kamalov and S. N. Yang, Phys. Rev. Lett. **83**, 4494 (1999).
[27] C. Mertz *et al.*, Phys. Rev. Lett. **86**, 2963 (2001).
[28] N. F. Sparveris *et al.*, Phys. Lett. B **651**, 102 (2007).